Journal of Magnetism and Magnetic Materials 373 (2015) 140–143

Contents lists available at ScienceDirect

Journal of Magnetism and Magnetic Materials

journal homepage: www.elsevier.com/locate/jmmm

Magnetic and structural properties of Co_2FeAl thin films grown on Si substrate

Mohamed Belmeguenai [a,*], Hanife Tuzcuoglu [a], Mihai Gabor [b], Traian Petrisor [b], Coriolan Tiusan [b,c], Dominique Berling [d], Fatih Zighem [a], Salim Mourad Chérif [a]

[a] LSPM (CNRS-UPR 3407) 99 Avenue Jean-Baptiste Clément Université Paris 13, 93430 Villetaneuse, France
[b] Center for Superconductivity, Spintronics and Surface Science, Technical University of Cluj-Napoca, Street Memorandumului No. 28, RO-400114 Cluj-Napoca, Romania
[c] Institut Jean Lamour, CNRS, Université de Nancy, BP 70239, F-54506 Vandœuvre, France
[d] IS2M (CNRS-LRC 7228), 15 rue Jean Starcky, Université de Haute-Alsace, BP 2488, 68057 Mulhouse-Cedex, France

ARTICLE INFO

Article history:
Received 21 November 2013
Received in revised form
24 January 2014
Accepted 3 February 2014
Available online 20 February 2014

Keywords:
Heusler alloy
Magnetic anisotropy
Ferromagnetic resonance
Magnetization dynamics

ABSTRACT

The correlation between magnetic and structural properties of Co_2FeAl (CFA) thin films of different thicknesses ($10\ nm < d < 100\ nm$) grown at room temperature on MgO-buffered Si/SiO_2 substrates and annealed at 600 °C has been studied. x-ray diffraction (XRD) measurements revealed an (011) out-of-plane textured growth of the films. The deduced lattice parameter increases with the film thickness. Moreover, pole figures showed no in-plane preferential growth orientation. The magneto-optical Kerr effect hysteresis loops showed the presence of a weak in-plane uniaxial anisotropy with a random easy axis direction. The coercive field, measured with the applied field along the easy axis direction, and the uniaxial anisotropy field increase linearly with the inverse of the CFA thickness. The microstrip line ferromagnetic resonance measurements for in-plane and perpendicular applied magnetic fields revealed that the effective magnetization and the uniaxial in-plane anisotropy field follow a linear variation versus the inverse CFA thickness. This allows deriving a perpendicular surface anisotropy coefficient of $-1.86\ erg/cm^2$.

1. Introduction

Heusler X_2YZ alloys [1,2] (X being a transition metal element, Y being another transition metal element and Z being a group III, IV, or V element) are an interesting class of materials due to their potential use as magnetic electrodes in giant and tunnel magnetoresistance devices used in magnetic memories (MRAM) [3], in low field magnetic sensors [4] and in microwave components for spintronic applications [5]. The most prominent representatives of the this kind of spintronic materials are Co-based full Heusler alloys due to their predicted half metallic character (magnetic materials that exhibit a 100% spin polarization rate at the Fermi level) even at room temperature and due to their high Curie temperature [6]. These make them ideal sources of high spin polarized currents to realize very large magnetoresistance values. Co_2FeAl (CFA) is one of the Co-based Heusler alloys having a very high Curie temperature (1000 K) and, theoretically predicted, a half-metallic character of their spin-split band structure. It can provide a giant tunneling magnetoresistance (360% at room temperature) [7] when used as an electrode in magnetic tunnel junctions, which makes CFA promising for practical applications. However, the crystalline structure and the chemical order of such materials strongly influence their magnetic and structural properties. Moreover, the substrate material, as well as the crystalline orientation of the substrate and the film thickness, have an impact on the magnetic anisotropy of magnetic thin films, such as CFA, because of the band hybridization and the spin–orbit interaction at the interface. Therefore, the correlation between their magnetic and structural properties and their dependence on film thicknesses, for precise control of the magnetic properties required by the integration of CFA as a magnetic electrode in spintronic devices, should be investigated. For this purpose, microstrip ferromagnetic resonance (MS-FMR), magneto-optical Kerr effect (MOKE) magnetometry and X-ray diffraction (XRD) techniques are used.

2. Sample preparation

CFA thin films of different thicknesses ($10\ nm < d < 100\ nm$) were grown on $Si(001)/SiO_2$ substrates using a magnetron sputtering system with a base pressure lower than 3×10^{-9} Torr. Prior to the deposition of the CFA films, a 4 nm thick MgO buffer layer was grown at room temperature (RT) by *rf* sputtering from a MgO

* Corresponding author.
E-mail address: belmeguenai.mohamed@univ-paris13.fr (M. Belmeguenai).

http://dx.doi.org/10.1016/j.jmmm.2014.02.014
0304-8853

polycrystalline target under an Argon pressure of 15 mTorr. Next, CFA thin films of different thicknesses were deposited at room temperature by dc sputtering under an Argon pressure of 1 mTorr, at a rate of 0.1 nm/s. Finally, the CFA films were capped with MgO (4 nm)/Ta(4 nm) bilayer.

Depending on sites occupied by the X, Y and Z atoms in the Heusler cell, different phases can be adopted by the Heusler alloys giving rise to chemical or atomic disorder. Heusler alloys with the totally ordered phase $L2_1$ transform into the B2 structure (when the Y and Z atoms randomly share their sites: Y–Z disorder). Moreover, they form an A2 structure when X, Y and Z randomly share all the sites. This chemical disorder strongly influences many of their physical properties. Indeed, it is reported by Picozzi that some types of disorder might lead to additional states at the Fermi level, thus reducing the spin polarization [8]. Furthermore, some Heusler alloys are amorphous in the as prepared state. Therefore, an annealing process is required to initiate the crystallization and to induce the atomic ordering for best Heusler alloys properties. After the growth of the stack, the structures were thus *ex-situ* annealed at 600 °C during 15 min in vacuum.

The structural properties of the samples have been characterized by XRD using a four-circle diffractometer. Their magnetic static and dynamic properties have been studied by magneto-optical Kerr effect magnetometer (MOKE) and microstrip ferromagnetic resonance (MS-FMR) [9], respectively.

3. Structural properties

The X-rays θ–2θ diffraction patterns for CFA thin films of different thicknesses revealed one peak which is attributed to the (022) diffraction line of CFA (Fig. 1a).

The lattice parameter (a), shown in Fig. 1b, increases with the increasing CFA thickness, similarly to samples grown on MgO substrates, where a direct correlation exists with the enhancement of the chemical order [10]. However, the lattice parameters remain smaller than the reported one in the bulk compound with the $L2_1$ structure (0.574 nm). Due to the overlap of the potential (002) CFA peak with the substrate reflections it is difficult to accurately evaluate de degree of chemical order in our films. Pole figures around the (022) type CFA peaks (Fig. 1c) indicate that the CFA films show a strong (011) fiber-texture with no in-plane preferential growth direction.

4. Magnetic properties

To analyze the experimental results, the total magnetic energy given by Eq. (1) is considered.

$$E = -M_s H[\sin\theta_M \sin\theta_H \cos(\varphi_M-\varphi_H) + \cos\theta_M \cos\theta_H] - (2\pi M_s^2 - K_\perp)\sin^2\theta_M - \frac{1}{2}(1+\cos 2(\varphi_M-\varphi_u))K_u \quad (1)$$

In the above expression φ_M (resp. φ_H) represents the in-plane (referring to the substrate edges) angle defining the direction of the magnetization M_s (resp. the external applied field H), while θ_M (resp. θ_H) is the out-of-plane angle between the magnetization (resp. the external field H) and the normal to the sample plane. φ_u defines the angles of the planar uniaxial anisotropy easy axis with respect to this substrate edge. K_u and $K_\perp$ are in-plane and out-of-plane uniaxial anisotropy constants, respectively.

For an in-plane applied magnetic field, the studied model provides the following expression (2) for the frequencies of the experimentally observable magnetic modes:

$$F_n^2 = \left(\frac{\gamma}{2\pi}\right)^2 \left[H\cos(\varphi_H-\varphi_M) + H_u\cos 2(\varphi_M-\varphi_u) + \frac{2A_{ex}}{M_s}\left(\frac{n\pi}{d}\right)^2\right] \times \left[H\cos(\varphi_H-\varphi_M) + 4\pi M_{eff} + \frac{H_u}{2_s}(1+\cos 2(\varphi_M-\varphi_u)) + \frac{2A_{ex}}{M_s}\left(\frac{n\pi}{d}\right)^2\right] \quad (2)$$

Where $(\gamma/2\pi) = g \times 1.397 \times 10^6$ Hz/Oe is the gyromagnetic factor.

We introduce the effective magnetization $M_{eff} = H_{eff}/4\pi$ obtained by:

$$4\pi M_{eff} = H_{eff} = 4\pi M_s - 2K_\perp / M_s = 4\pi M_s - H_\perp \quad (3)$$

As experimentally observed, the effective perpendicular anisotropy term $K_\perp$ (and, consequently, the effective perpendicular anisotropy field $H_\perp$) is thickness dependent. $K_\perp$ describes an effective perpendicular anisotropy term which writes as:

$$K_\perp = K_{\perp v} + 2K_{\perp s}/d \quad (4)$$

where $K_{\perp s}$ refers to the perpendicular anisotropy term of the interfacial energy density. Finally we define $H_u = 2K_u/M_s$ as the in-plane uniaxial anisotropy field. The uniform precession mode corresponds to $n=0$. The other modes to be considered (perpendicular standing modes: PSSW) are connected to integer values of n: their frequencies depend upon the exchange stiffness constant A_{ex} and upon the film thickness d.

In the case of an out-of-plane perpendicular applied magnetic field, the precession frequency is given by:

$$F_\perp = \left(\frac{\gamma}{2\pi}\right)\left[H - 4\pi M_{eff} + \frac{2A_{ex}}{M_s}\left(\frac{n\pi}{d}\right)^2\right] \quad (5)$$

4.1. Static properties

The average magnetization at saturation measured by vibrating sample magnetometer at room temperature for all samples has been found to be $M_s = 1000 \pm 50$ emu/cm^3. The typical MOKE hysteresis loops, measured versus external magnetic field directions with respect to one of the substrate edges for all the samples, are represented in Fig. 2a for the 50 nm thick film. The shape of

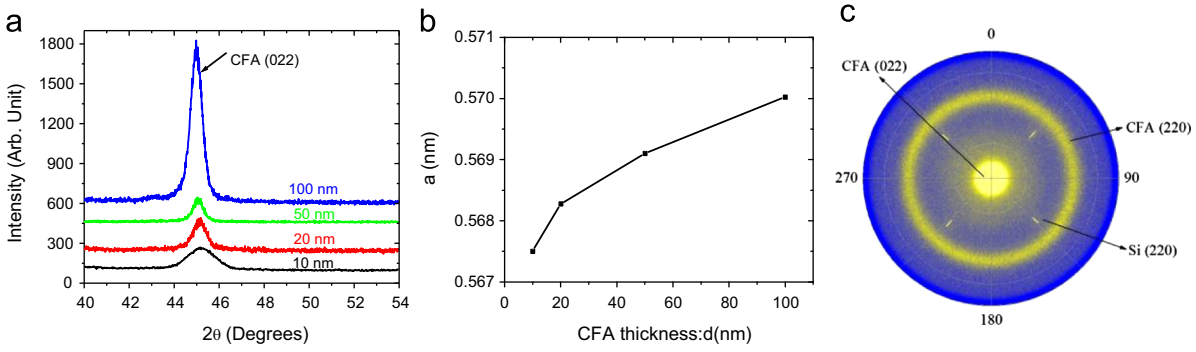

Fig. 1. Thickness dependence of (a) θ–2θ patterns (b) lattice parameter; and (c) pole figure around a (022) peak of 50 nm thick CFA film.

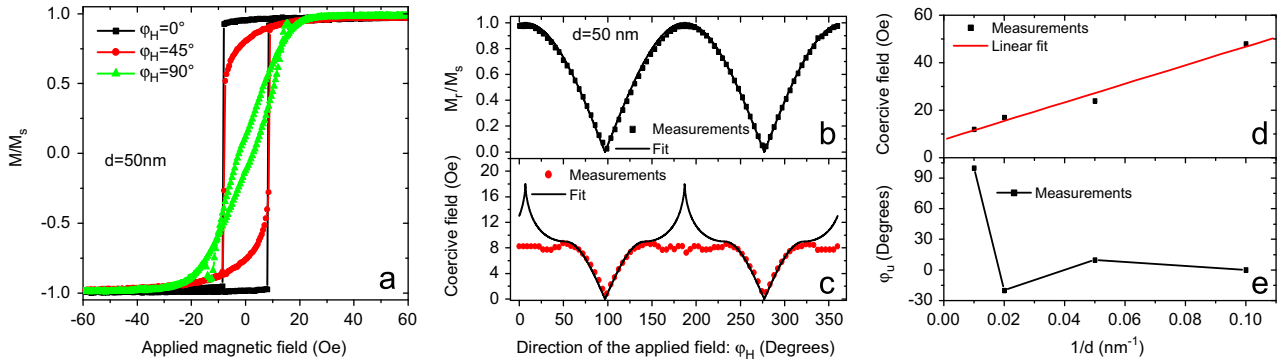

Fig. 2. (a) MOKE hysteresis loops and the corresponding angular dependences of (b) the normalized remanent magnetization (c) the coercive field of the 50 nm thick Co_2FeAl thin film. (d) and (e) thickness dependence of the easy coercive field and the magnetization easy axis direction (φ_u), respectively of the Co_2FeAl thin films.

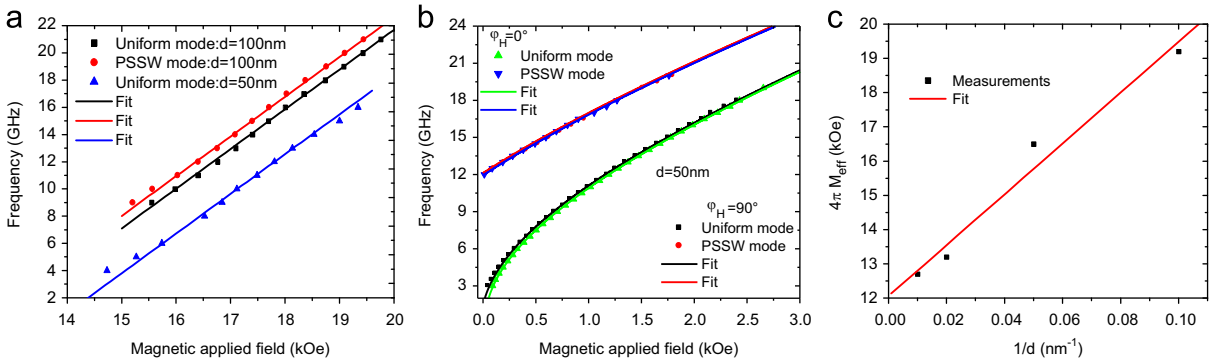

Fig. 3. Uniform precession and perpendicular standing spin wave (PSSW) modes frequencies versus the (a) perpendicular and (b) in-plane applied magnetic fields for 100 and 50 nm thick Co_2FeAl thin films. The solid lines refer to the fit using the above mentioned model. (c) Thickness dependence of the effective magnetization of Co_2FeAl thin films deduced from the MS-FMR measurements.

the magnetization reversal loops changes with the magnetic field orientation mainly due to the uniaxial magnetic anisotropy. The corresponding typical angular dependence of coercive fields (H_C) and normalized remanent magnetizations (M_r/M_s) are represented in Fig. 2b and c for the 50 nm thick film. The samples have a similar angular dependence of H_C and M_r/M_s however, the H_C magnitude and the easy axis directions are different from each other (Fig. 2d and e). Apparently, the angular dependences agree with those of Stoner Wohlfarth (coherent rotation: CR) model as shown in Fig. 2b and c. Despite of the perfect agreement for M_r/M_s, a significant discrepancy for H_C is shown around the easy axis direction between the CR model and measurements. In fact, the coercive fields deduced from the magnetization loops around the easy axis are smaller than the one obtained from CR model since that they are usually determined by domain nucleation and sample imperfection.

The coercive field deducted from hysteresis loops obtained for a magnetic field applied along the direction of the easy axis, are shown in Fig. 2d as a function of the inverse film thickness. H_C increases linearly with the inverse of the film thickness maybe due to the enhancement of the chemical order as the thickness increases.

4.2. Dynamic properties

The MS-FMR spectra measured for in-plane and perpendicular applied magnetic fields show the existence of a uniform mode for all samples and a first perpendicular standing spin wave mode only for the thickest films (100 and 50 nm thick films). Typical field dependences of resonance frequencies of the uniform precession and the first PSSW modes are shown in Fig. 3a and b, respectively for magnetic fields applied in-plane and perpendicular to the CFA film plane of various thicknesses. By fitting the data in Fig. 3 to the above presented model, the gyromagnetic factor (γ), exchange stiffness constant (A_{ex}) and the effective magnetization ($4\pi M_{eff}$) are extracted. The fitted γ and A_{ex} values are found to be constant across different samples and equal to 29.2 GHz/T and 1.5 μerg/cm, respectively. This exchange constant value is in good agreement with that indicated by Trudel et al. [6].

Interestingly, the extracted effective magnetization from the MS-FMR measurements, shown in Fig. 3c follows a linear variation versus the inverse CFA thickness. The linear fit of the measurements allows to determine the value of the perpendicular surface anisotropy constant: $K_{\perp s} = -1.86$ erg/cm^2. The $4\pi M_{eff}$ value when d tends to infinity, equal to 12.05 kOe, is very close to the M_s mentioned above, taking into account the experimental accuracy. This value of the surface perpendicular anisotropy constant is within the range (1.3 erg/cm^2 [11] and 1.8 erg/cm^2 [12]), but of an opposite sign, of those reported in the MgO-based magnetic tunnel junctions having CoFeB electrodes or in Ta/CFA/MgO multilayers [13]. Ikeda et al. [11] attributed this perpendicular anisotropy in the Ta/CoFeB/MgO structure to the contribution of the CoFeB/MgO interface. Wang et al. [14] have also argued that this anisotropy is due to the CoFeB/MgO interface based on the fact that it is only observed when the MgO thickness overpasses 1 nm. Therefore, we conclude that the uniaxial perpendicular anisotropy derives from a surface energy term. Its negative value favors in-plane orientation of the magnetization. The origin of this anisotropy is most likely due to the CFA/MgO interface. This was confirmed (note shown here) by measuring the effective magnetization of a 10 nm CFA thick layer deposited on a $SrTiO_3$ substrate by using a 3 nm CoFe thick buffer layer where a $4\pi M_{eff} = 12.5$ kOe has been measured.

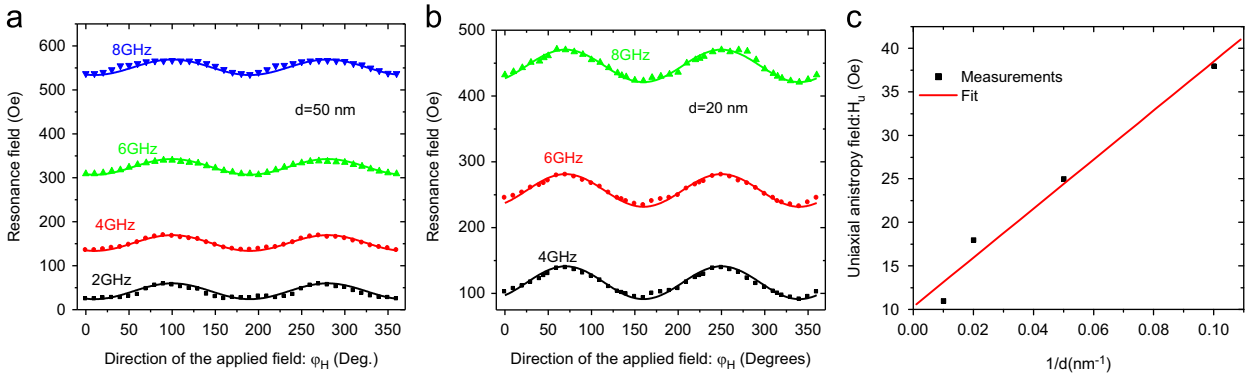

Fig. 4. Angular dependence of the resonance field of (a) 50 nm and (b) 20 nm thick Co_2FeAl thin films. The solid lines refer to the fit using the above mentioned models. (c) Thickness dependence of the uniaxial (H_u) extracted from the fit of MS-FMR measurements. The solid lines are the linear fits.

Fig. 4a and b shows the typical MS-FMR angular dependence of the resonance field at different frequencies for 20 and 50 nm thick films. The MS-FMR measurements show that the angular behavior of resonance fields is governed by the term of uniaxial anisotropy. The uniaxial anisotropy field, presented in Fig. 4c, shows a similar behavior as the coercive field and increases linearly with the CFA inverse thickness. This uniaxial anisotropy is maybe due to the substrate vicinal structure induced by the miscut. However, the easy direction of the uniaxial anisotropy, determined with a 90° precision since it is referenced with a respect to substrate edges, changes with the thickness (Fig. 2e) and complicates the identification of its origin. Therefore, a completely satisfactory interpretation of the presence of H_u and its thickness dependence is still missing. Assuming that this thickness dependence is due to uniaxial surface anisotropy ($H_u = H_{uv} + 4K_{us}/M_s$), the uniaxial surface anisotropy constant estimated from the linear fit of uniaxial anisotropy field is $K_{us} = 7 \times 10^{-3}$ erg/cm^2. For CFA films grown on Si substrates, the absence of the in-plane fourfold anisotropy, observed in the case of CFA thin films deposited on MgO [10,15], is in good agreement with the above-mentioned in-plane random orientation growth of the CFA films grown on Si substrates. For all the samples, the obtained values of the magnetic parameters corresponding to the best fits of the MS-FMR measurements have been used to fit the MOKE measurements where a good agreement has been obtained.

5. Conclusion

Co_2FeAl films of various thicknesses ($10\ \text{nm} \leq d \leq 100\ \text{nm}$) were prepared by sputtering on Si(001) substrates and annealed at 600 °C. XRD measurements revealed an (011) out-of-plane textured growth of the films with no in-plane preferential growth orientation. The lattice parameter increases with increasing CFA thickness, probably due to the enhancement of the chemical order. MOKE hysteresis loops obtained with different field orientations revealed that the easy axis coercive field varies linearly with the inverse CFA thickness. The microstrip ferromagnetic resonance has been used to study the dynamic properties. The angular and the field dependences of the resonance field and frequency, respectively, have been analyzed through a model based on a magnetic energy density which, in addition to Zeeman, demagnetizing and exchange terms, is characterized by a uniaxial anisotropy to determine the most relevant parameters. The in-plane uniaxial anisotropy field, present in all the samples, increases linearly with the inverse CFA thickness. However, the uniaxial anisotropy easy axis direction changes with the thickness. The effective magnetization shows drastically linear increase with the inverse CFA thickness suggesting a surface anisotropy induced by the CFA/MgO interface.

Acknowledgments

This work was partially supported by POS CCE Project ID 574, code SMIS-CSNR 12467 and CNCSIS UEFISCSU Project no. PNII IDEI 4/2010 code ID-106.

References

[1] H.C. Kandpal, G.H. Fecher, C. Felser, J. Phys. D 40 (2007) 1507.
[2] R.A. de Groot, F.M. Mueller, P.G. van Engen, K.H.J. Buschow, Phys. Rev. Lett. 50 (1983) 2024.
[3] R.W. Dave, G. Steiner, J.M. Slaughter, J.J. Sun, B. Craigo, S. Pietambaram, K. Smith, G. Grynkewich, M. DeHerrera, J. Åkerman, S. Tehrani, IEEE Trans. Magn. 42 (2006) 1935.
[4] P.P. Freitas, R. Ferreira, S. Cardoso, F. Cardoso, J. Phys.: Condens. Matter 19 (2007) 165221.
[5] A.A. Tulapurkar, Y. Suzuki, A. Fukushima, H. Kubota1, H. Maehara, K. Tsunekawa, D.D. Djayaprawira, N. Watanabe, S. Yuasa, Nature 438 (2005) 339.
[6] S. Trudel, O. Gaier, J. Hamrle, B. Hillebrands, J. Phys. D 43 (2010) 193001.
[7] W.H. Wang, H. Sukegawa, K. Inomata, Phys. Rev. B 82 (2010) 092402.
[8] S. Picozzi, A. Continenza, A.J. Freeman, Phys. Rev. B 69 (2004) 094423.
[9] M. Belmeguenai, F. Zighem, Y. Roussigné, S.-M. Chérif, P. Moch, K. Westerholt, G. Woltersdorf, G. Bayreuther, Phys. Rev. B 79 (2009) 024419.
[10] M. Belmeguenai, H. Tuzcuoglu, M.S. Gabor, T. Petrisor , C. Tiusan, D. Berling, F. Zighem, T. Chauveau, S.M. Chérif, P. Moch, Phys. Rev. B 87 (2013) 184431.
[11] S. Ikeda, K. Miura, H. Yamamoto, K. Mizunuma, H.D. Gan., M. Endo, S. Kanai, J. Hayakawa, F. Matsukura, H. Ohno, Nat. Mater. 9 (2010) 721.
[12] D.C. Worledge, G. Hu, D.W. Abraham, J.Z. Sun, P.L. Trouilloud, J. Nowak, S. Brown, M.C. Gaidis, E.J. O'Sullivan, R.P. Robertazzi, Appl. Phys. Lett. 98 (2011) 022501.
[13] M.S. Gabor, T. Petrisor , C. Tiusan, T. Petrisor, J. Appl. Phys. 114 (2013) 063905.
[14] W.G. Wang, M. Li, S. Hageman, C.L. Chien, Nat. Mater. 11 (2012) 64.
[15] M.S. Gabor, T. Petrisor , C. Tiusan, M. Hehn, T. Petrisor, Phys. Rev. B 84 (2011) 134413.